CERN

LHCb Collaboration

Comparison of $B_s^0 \to D_s^- \mu^+ \nu_\mu$ and $B^0 \to D^- \mu^+ \nu_\mu$ to test SU(3) symmetry

Author:
Veronica S. Kirsebom

Supervisors:
Dr. Mirco Dorigo &
Dr. Melody R. Salzgeber

August 31, 2017

Contents

1 Introduction to semileptonic $B^0_{(s)} \to D^-_{(s)}\mu^+\nu_\mu$ Decays

The purpose of this summer student project has been to perform the first step towards a test of SU(3) symmetry by comparing the form factors of the two semileptonic decays:

$$B^0_s \to D^-_s \mu^+ \nu_\mu \qquad (\bar{B}^0_s \to D^+_s \mu^- \nu_\mu) \tag{1}$$
$$B^0 \to D^- \mu^+ \nu_\mu \qquad (\bar{B}^0 \to D^+ \mu^- \nu_\mu) \tag{2}$$

In both decays the b quark of the B meson is decaying into a c quark and thereby transforming the B meson into a D meson. The W boson emitted in the weak decay of the b quark decays into a μ and ν_μ as illustrated in Fig. 1. The only difference between the two decays is the spectator quark, which for $B_s \to D^-_s$ is a s quark and for $B^0 \to D^-$ is a d quark as illustrated in Fig. 1a and Fig. 1b respectively. Assuming SU(3) symmetry is not violated i.e. the mass differences between u, d and s quarks can be neglected [2], the form factors, which accounts for the effects of the strong interaction between the bound quarks, would be expected to be the same for $B_s \to D^-_s$ and $B^0 \to D^-$.

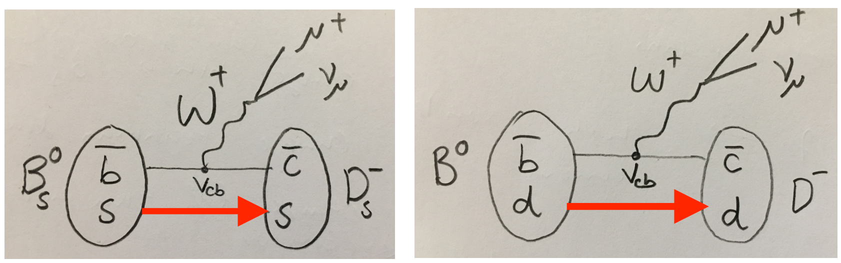

(a) Feynman diagram of the decay $B^0_s \to D^-_s \mu^+ \nu_\mu$

(b) Feynman diagram of the decay $B^0 \to D^- \mu^+ \nu_\mu$

Figure 1

1.1 Measuring form factors using $P_\perp(D)$

The form factor for $B^0_{(s)} \to D^-_{(s)}\mu^+\nu_\mu$ is a function of the transfer momentum of the W boson, q^2, and it is parametrised as an expansion of a parameter, ρ^2 [3]. Since the neutrino cannot be detected q^2 is only partially reconstructed and this creates a challenge for measuring the form factors. One can approximate the value of q^2 by imposing energy-momentum conservation and by assuming the missing momentum to be only due to a single neutrino. In this calculation one obtain a second order equation for the longitudinal component $p_{\nu\|}$, of the neutrino momentum with respect to the B meson flight direction leading to an ambiguity in q^2. The standard approach to this problem is to compute $p_{\nu\|}$ and try to develop strategies for obtaining the correct solution. However, in general this approach leads to a poor resolution of the measurement.

In this project we have therefore chosen an alternative approach to extract the form factors of these decays. The idea is to use another variable, which is correlated with q^2 and which we can fully reconstruct. A variable which satisfies these criteria is $P_\perp(D)$, which is the perpendicular component of the D meson momentum with respect to the flight direction of the B meson, as illustrated in Fig. 2a.

The relation between $P_\perp(D)$ and q^2 can be obtained from simulation, which allow us to fully reconstruct both variables (see Fig. 2b). The sensitivity of $P_\perp(D)$ to the form factor parameter can be tested by simulating $B^0 \to D^-\mu^+\nu_\mu$ decay for different values of ρ^2 ranging from approximately $1/3\rho^2_{nom}$ to $5/3\rho^2_{nom}$, where $\rho^2_{nom} = 1.18$ is the nominal value [4]. As expected the shape of the q^2 changes significantly for different values of ρ^2 (see Fig. 2c). Although the change in $P_\perp(D)$ is not as dramatic it is indeed changing (see Fig. 2d) suggesting $P_\perp(D)$ can be used to extract the form factor parameter ρ^2.

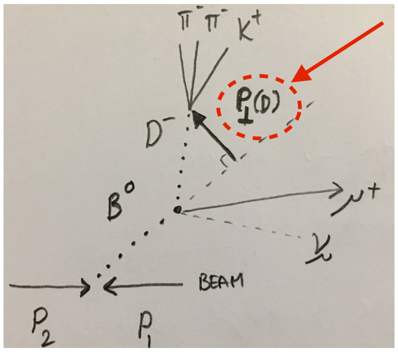

(a) The variable $P_{\perp}(D)$ in the B meson decay

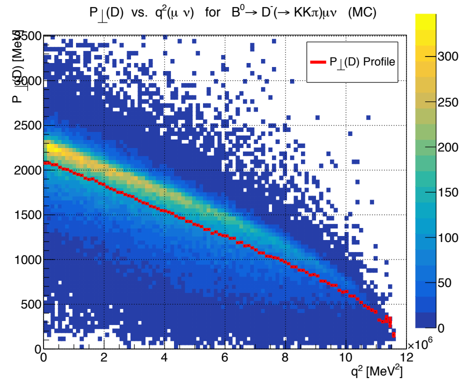

(b) 2D histogram of $P_{\perp}(D)$ and q^2 from MC generated $B_s^0 \to D_s^- \mu^+ \nu_\mu$ decays

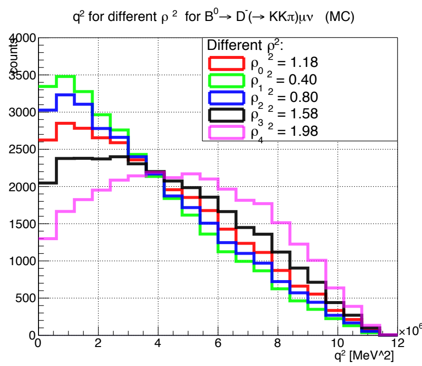

(c) MC q^2 distribution for different ρ^2 values

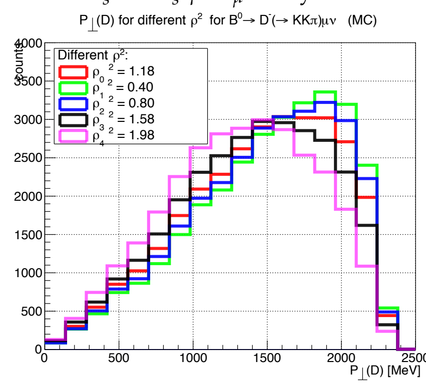

(d) MC $P_{\perp}(D)$ distribution for different ρ^2 values

Figure 2

2 Analysis goal and strategy

The goal of this analysis is to determine $P_{\perp}(D)$ distribution for $B_s^0 \to D_s^- \mu^+ \nu_\mu$ and $B^0 \to D^- \mu^+ \nu_\mu$ and finally compare them in order to test SU(3) symmetry. The strategy is as follows:

1. Split data sample in bins of the variable $P_{\perp}(D)$
2. Perform a fit to the corrected B mass in each bin to obtain signal yields and thereby the distributions $P_{\perp}(D)(B_s^0 \to D_s^- \mu^+ \nu_\mu)$ and $P_{\perp}(D)(B^0 \to D^- \mu^+ \nu_\mu)$.
3. Finally compute the ratio: $P_{\perp}(D)(B_s^0 \to D_s^- \mu^+ \nu_\mu)/P_{\perp}(D)(B^0 \to D^- \mu^+ \nu_\mu)$ in order to test SU(3) symmetry in $B_s^0 \to D_s^-$ and $B^0 \to D^-$

2.1 Data sample

The data used for this analysis is collected by the LHCb experiment in run 1 at $\sqrt{s} = 7 - 8$ TeV and correspond to an integrated luminosity of 3 fb^{-1}. The selected data samples has been inherited from B_s^0 and D_s lifetime measurement [1]. The number of opposite and same sign candidates are found in table 1. The opposite sign data (OS) are real candidates whereas the same sign data (SS) are unphysical candidates where a B meson is reconstructed from a D meson and μ of same charge. The SS data is used to model the combinatorial background. In order to get samples of large statistics the final states of D_s^- and D^- are chosen to be the cabibbo favoured decays to $K^+K^-\pi^-$ and $K^+\pi^-\pi^-$ respectively.

Decay	OS	SS
$B^0 \to D\mu\nu$	2,611,001	28,767
$B_s^0 \to D_s\mu\nu$	467,951	14,228

Table 1: Number of candidates after selected

2.2 Corrected B mass fit

Usually, the invariant mass of the final-state products is used to reconstruct the signal of the parent particle; however, in our case the decays are only partially reconstructed leading to a broadened B mass distribution composed of several components. Instead of using the visible mass of the B meson, i.e. the invariant of $KK\pi\mu$ and $K\pi\pi\mu$ system, we use the so-called corrected mass [1], which compensates for parts of the missing momentum and makes the mass distribution more narrow, helping to distinguish the different components. The corrected mass is given by:

$$m_{corr} = p_{\perp,D\mu} + \sqrt{m_{D\mu}^2 + p_{\perp,D\mu}^2} \tag{3}$$

where $m_{D\mu}$ is the invariant mass of the $D\mu$ system and $p_{\perp,D\mu}$ is the momentum of the $D\mu$ system transverse to the flight direction of the B meson.

In order to discriminate signal from background and determine the signal composition a binned least-square fit to the corrected B mass is used. The fit minimizes the χ^2 variable given by:

$$\chi^2 = \sum_{i=1}^{bins} \frac{(n_i - p_i(\theta))^2}{\sigma_{ni}^2 + \sigma_{pi}^2(\theta)} \tag{4}$$

where n_i and p_i is the number of observed and predicted candidates with statistical uncertainties σ_{ni} and σ_{pi} in mass bin i [1].

Mass shapes for the components are obtained from simulations except the combinatorial background, which is obtained from SS data.

2.3 Analysis of $B^0 \to D^-\mu^+\nu_\mu$ decay

From the analysis of B_s^0 and D_s lifetime measurement [1] the expected composition of the signal is:

1. $B^0 \to D^-\mu^+\nu_\mu$ (signal)
2. $B^0 \to D^{*-}\mu^+\nu_\mu$
3. $B^0 \to D^{**-}\mu^+\nu_\mu$ (i.e. all the semimuonic decays of the B^0 meson not included in the two first categories)
4. $B^0 \to D^-\tau^+\nu_\mu X$ (with the $\tau \to \mu\nu\nu$)
5. $B^+ \to D^-\mu^+\nu_\mu X$
6. Combinatorial (SS data) .

where "X" denotes all decay products, which are not measured.

The fit method is verified by fitting the integrated sample of $B^0 \to D^-\mu^+\nu_\nu$ and comparing it to previous analysis [1]. The mass shapes of the components must be sufficiently different for the fit to be able to distinguish them. The fit is not able to distinguish the mass shapes of $B^0 \to D^{**-}\mu^+\nu_\mu$ and $B^+ \to D^-\mu^+\nu_\mu X$ and they are therefore summed together into one single template called $B^0/B^+ \to D^-\mu^+\nu X$ using their respective fractions obtained from simulation. The result of the fit is good with a χ^2/ndf = 109.6/88 and a probability of 0.059 (see Fig. 3a). The signal contribution is found to be the dominant one $(49.18\% \pm 0.54\%)$, whereas the contribution from $B^0 \to D^-\tau^+\nu_\mu X$ is found to be negligible $(1.26\% \pm 0.77\%)$ and it is therefore not used in the following analysis.

The next step is to split the sample into bins of $P_\perp(D)$, which will change the ratio and the mass shapes of the components in each bin with respect to the integrated sample. The splitting seeks to maximise the differences between mass shapes for signal and background in each bin. The sample is split into the six following intervals of $P_\perp(D)$ measured in MeV: bin1: [0, 812], bin2: [812, 1155], bin3: [1155,1460], bin4: [1460,1795], bin5: [1795, 2150] and bin6: [2150,4500].

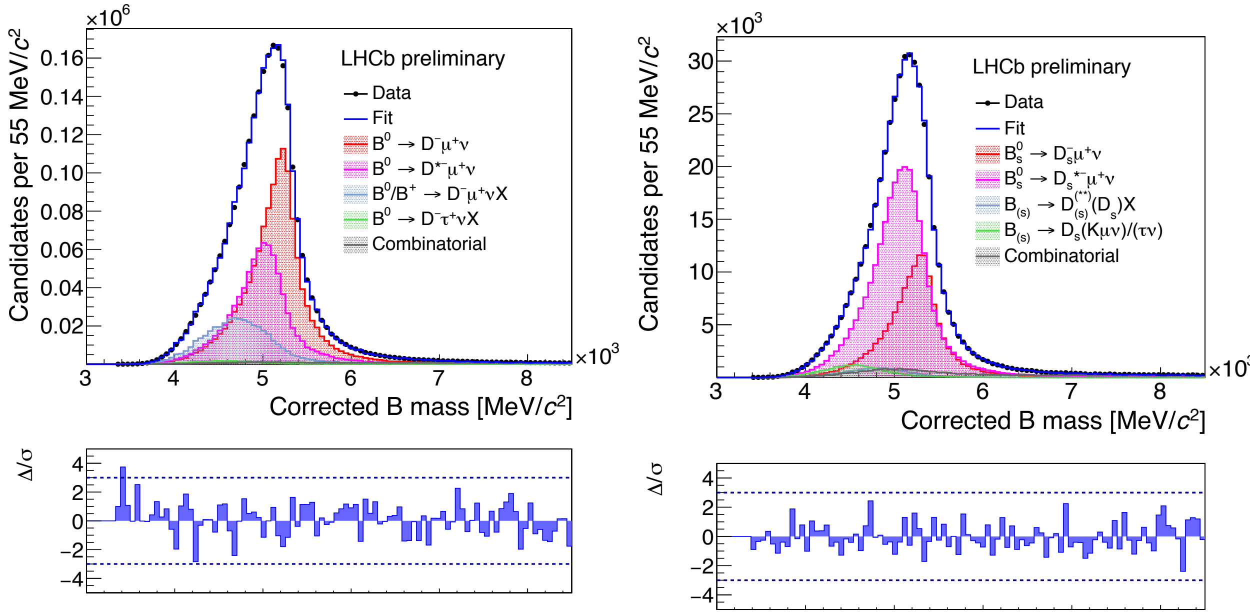

(a) Fit result for the integrated $B^0 \to D^- \mu^+ \nu_\nu$ sample

(b) Fit result for the integrated $B_s^0 \to D_s^- \mu^+ \nu_\nu$ sample

Figure 3

2.3.1 Preliminary $P_\perp(D)$ distribution for $B^0 \to D^- \mu^+ \nu$

In each bin of $P_\perp(D)$ the yield for $B^0 \to D^- \mu^+ \nu_\mu$ is found by performing the corrected mass fit. In bin 5 the fit cannot distinguish the two components $B^0/B^+ \to D^- \mu^+ \nu X$ and $B^0 \to D^{*-} \mu^+ \nu_\mu$, so they are summed together in one template. The result of the fit in each bin can be seen in Fig. A.1 in appendix A. The yield of the signal obtained from the fit is used to construct $P_\perp(D)$ distribution, which is shown in fig. 4a together with the expectation from simulation. The agreement between data and MC is good with χ^2/dof=4.90/5 and a probability of 0.43.

2.4 Analysis for $B_s^0 \to D_s^- \mu^+ \nu_\mu$ decay

The expected composition of B_s^0 is more complicated than for B^0. However, it turns out that many of the background components can be summed into one of two background templates resulting in the following five components:

1. $B_s^0 \to D_s^- \mu^+ \nu_\mu$ (signal)
2. $B_s^0 \to D_s^{*-} \mu^+ \nu_\mu$
3. $D_{(s)}^{**}(D_s)X$ (sum of: $B^0 \to D^{(*)-} D_s^{(*)+}$, $B^+ \to D^{(*)0} D_s^{(*)+}$, $\Lambda_b^0 \to \Lambda_c^+ D_s^{(*)+}(\pi^0)$, $B_s \to D^{(*)-} D_s^{(*)+}$)
4. $D_s(K\mu\nu)/(\tau\nu)$ (sum of: $B^- \to D_s^{*+} K^- \mu^- X$, $B^0 \to D_s^{(*)-} K_s^0 \mu^+ X$, $B_s^0 \to D_s^- \tau^+(\to \mu^+ \nu\nu)\nu X$)
5. Combinatorial background.

The fit method is also verified for $B_s^0 \to D_s^- \mu^+ \nu_\nu$ by fitting the integrated sample of $B_s^0 \to D_s^- \mu^+ \nu_\nu$ and comparing it to previous analysis [1]. The result of the fit is good with a $\chi^2/ndf = 84.01/89$ and a probability of 0.63 (see Fig. 3b). The dominant contribution is found to be $B_s^0 \to D_s^{*-} \mu^+ \nu_\mu$ ($57.9\% \pm 0.886\%$) while the second largest contribution is the signal ($29.2\% \pm 0.518\%$).

2.4.1 Preliminary $P_\perp(D)$ distribution for $B_s^0 \to D_s^- \mu^+ \nu$

The analysis of B_s^0 is the same as for B^0 and so the yield of $B_s^0 \to D_s^- \mu^+ \nu_\mu$ in each of the six bins are found by performing the corrected mass fit in each bin. The components $D_{(s)}^{**}(D_s)X$ and $D_s(K\mu\nu)/(\tau\nu)$ turn out to be indistinguishable for the fit and consequently they are summed together in one template $D_{(s)}^{**}(D_s)X/D_s(K\mu\nu)/(\tau\nu)$.

The result of the fit in each bin can be seen in Fig. 1 of appendix B. The yield of the signal obtained from the fit is used to extract $P_\perp(D)$ distribution shown in fig. 4b together with the expectation from MC simulation generated under the assumption of perfect SU(3) symmetry. The agreement between data and MC is not good with $\chi^2/dof = 29.8/5$ and a probability of $1.6 \cdot 10^{-5}$. The largest disagreement is found in bin 5 and 3, however, systematic uncertainties have to be considered before any conclusion can be made.

2.5 Preliminary comparison of $P_\perp(D)(B_s^0 \to D_s^- \mu^+ \nu_\mu)$ and $P_\perp(D)(B^0 \to D^- \mu^+ \nu_\mu)$

The preliminary comparison of $P_\perp(D)(B_s^0 \to D_s^- \mu^+ \nu_\mu)$ and $P_\perp(D)(B^0 \to D^- \mu^+ \nu_\mu)$ is shown in fig. 4c together with the expectation from MC. This is the first step toward a test of SU(3) symmetry between $B_s^0 \to D_s^-$ and $B^0 \to D^-$. More work is still needed and systematic uncertainties have to be taken into account before a meaningful comparison of the two distributions can be made.

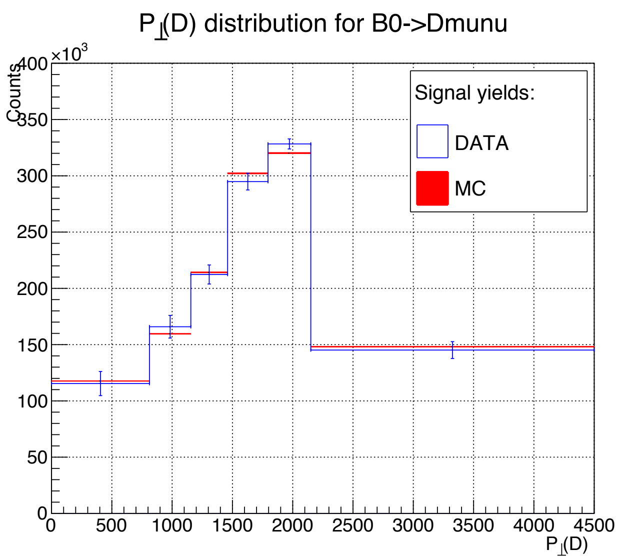

(a) $P_\perp$ distribution for $B^0 \to D^- \mu^+ \nu_\mu$

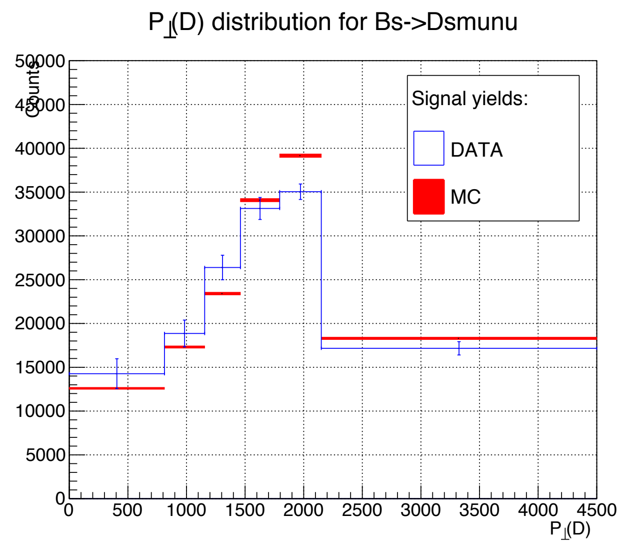

(b) $P_\perp$ distribution for $B_s^0 \to D_s^- \mu^+ \nu_\mu$

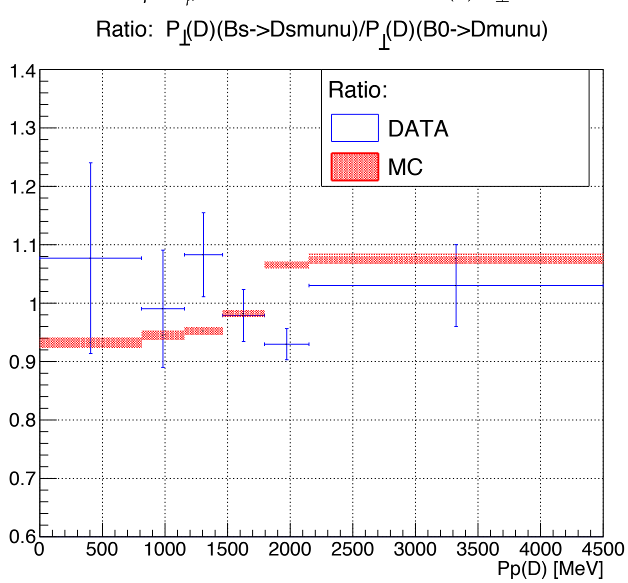

(c) Ratio of $P_\perp(B_s^0 \to D_s^- \mu^+ \nu_\mu)$ and $P_\perp(B^0 \to D^- \mu^+ \nu_\mu)$ distributions

3 Conclusion and outlook

We have made the first attempt to compare $B_s^0 \to D_s^- \mu^+ \nu_\mu$ and $B^0 \to D^- \mu^+ \nu_\mu$ decays to test SU(3) symmetry. In our analysis we have proven that we can extract the $P_\perp(D)$ distribution of $B \to D\mu\nu$ decays and we have validated this method on the known B^0 sample. More work is still needed on the analysis of B_s^0 in order to test SU(3), but the method looks already promising. Next step would be to extract the form factor parameter ρ^2 from a fit to the ratio of $P_\perp(D)$ distributions and to add data collected by LHCb in run 2.

Appendices

Appendix A

Corrected mass fit results for the split sample of $B^0 \to D^- \mu^+ \nu_\mu$

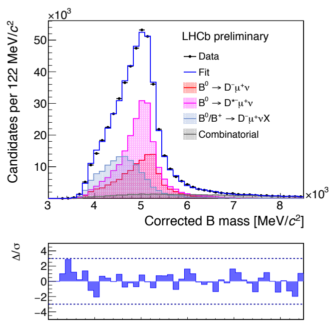

(a) bin1

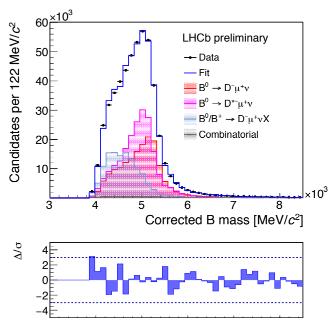

(b) bin2

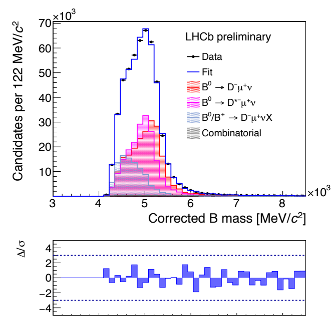

(c) bin3

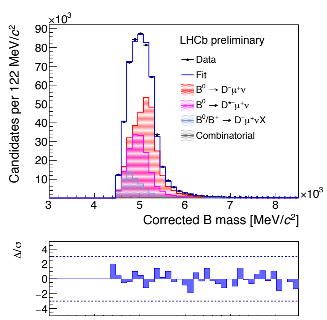

(d) bin4

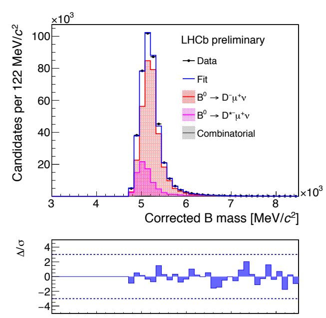

(e) bin5

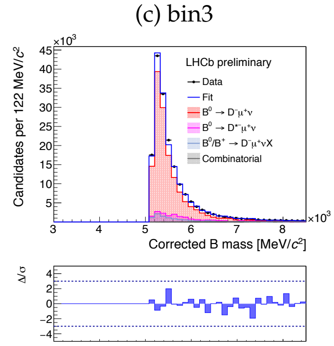

(f) bin6

Figure A.1: Corrected mass fit result in each bin for $B^0 \to D^- \mu^+ \nu_\mu$

Appendix B

Corrected mass fit results for the split sample of $B_s^0 \to D_s^- \mu^+ \nu_\mu$

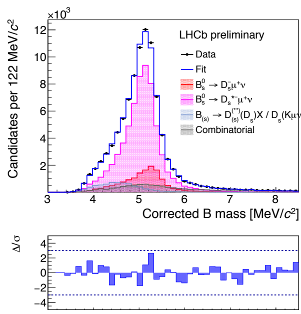

(a) bin1

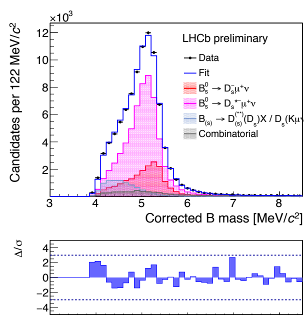

(b) bin2

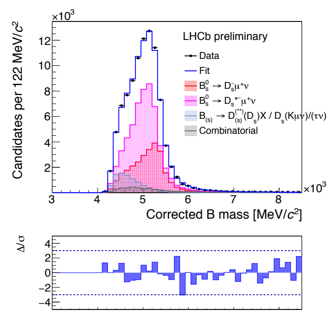

(c) bin3

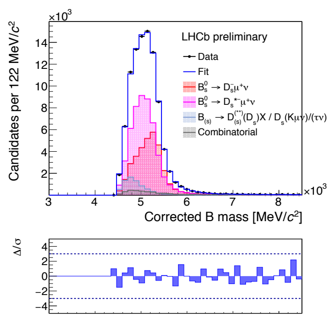

(d) bin4

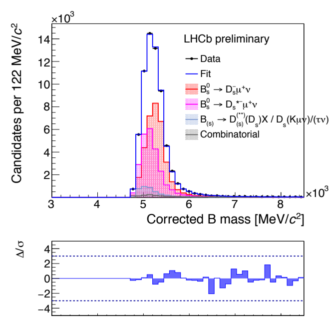

(e) bin5

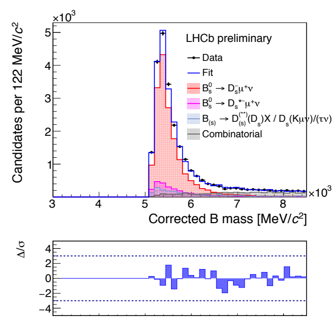

(f) bin6

Figure 1: Corrected mass fit result in each bin for $B_s^0 \to D_s^- \mu^+ \nu_\mu$

Bibliography

[1] T. J. Boettcher, A. Di Canto, M. Dorigo, B. Maurin, and D. Tonelli. *Measurement of the decay-width difference between the* B_s^0 *and* B_0 *mesons and the Ds and D mesons*. LHCb-ANA-2016-068, CERN & EPFL, March 7. 2017.

[2] M. Thomson. *Modern Particle Physics, chapter 9*. Cambridge University Press, 2013.

[3] M. Neubert. *Heavy-quark symmetry*. Stanford University, Physics Reports 245 (1994) 259-393.

[4] Y. Amhis et al., *Averages of b-hadron, c-hadron, and tau-lepton properties as of summer 2016*, arXiv:1612.07233, 2016.